Nail Abnormality Identification Using Roboflow and Yolov8

Rosemarie V Pellegrino
Mapua University
Philippines
rpellegrino@mapua.edu.ph

Jethro Hoyt T. Lacuesta
Mapua University
Philippines
jhtlacuesta@mymail.mapua.edu.ph

Carl Ferione L. Dela Cuesta
Mapua University
Philippines
cfldelacuesta@mymail.mapua.edu.ph

Abstract

This study focuses on the automation of the Clotting Time coagulation test through the use of image processing. Image to be processed will be taken from the Arduino Yun which serves as a frame grabber of the system. Through the obtained Clotting Time, dosage measurement of Warfarin will be given. Dosage measurement was done by using the Two-Step Dosing Algorithm which monitors patients undergoing Warfarin therapy. The algorithm makes use of the patient's computed INR to give off the corresponding dosage. INR is the quotient of the abnormal Clotting Time and mean of normal Clotting time. Error percentage was conducted to prove the system's ability to accurately determine a patient's Clotting Time.

CCS Concepts

• **Applied Computing**; • **Life and Medical Sciences**; • **Computational biology**; • **Imaging**;

Keywords

INR, arduino yun, coagulation, warfarin therapy, automation

ACM Reference Format:
Rosemarie V Pellegrino, Jethro Hoyt T. Lacuesta, and Carl Ferione L. Dela Cuesta. 2024. Nail Abnormality Identification Using Roboflow and Yolov8. In *2024 14th International Conference on Biomedical Engineering and Technology (ICBET 2024), June 14–17, 2024, Seoul, Republic of Korea.* ACM, New York, NY, USA, 7 pages. https://doi.org/10.1145/3678935.3678956

1 INTRODUCTION

In recent years, the field of medical image analysis has witnessed remarkable advancements with the integration of deep learning techniques. One area that has seen significant interest is dermatology, where the early and accurate identification of various skin conditions can play a crucial role in disease management and treatment. Nail abnormalities, in particular, have been recognized as valuable indicators of several systemic and dermatological disorders [1]. Timely diagnosis of nail abnormalities can lead to early intervention, potentially improving patient outcomes and quality of life [2].

Traditional methods of nail abnormality identification relied heavily on manual inspection by dermatologists, which can be time-consuming, subject to human error, and limited by the experience of the practitioner [3]. However, recent breakthroughs in computer vision and deep learning offer a promising solution to automate this process efficiently and accurately. Among the cutting-edge deep learning models, YOLOv8 (You Only Look Once version 8) stands out as a powerful and versatile object detection algorithm known for its real-time performance and robustness [4], [5].

Although this process has been extensively studied, some studies have revealed that the absence of a known set of data often makes it more difficult to identify abnormal human nails. In this specific application, fine-tuning machine learning models could be challenging due to the potential for inadequate image quality [6], [7]. Nonetheless, it's important to note that the YOLO framework's background has been extensively used and proven effective in various fields [8-17].

The following objectives are explicitly stated in the proposed research: (1) this study aims to model the nail abnormality identification using a custom dataset which includes Terry's nails, Splinter haemorrhage, and Spoon nail. (2) to use Roboflow and Yolov8 to train and test the device using validated images. (3) evaluate different augmentation types (image-level, Bounding-box level, and Color-level) on instance segmentation.

Identifying nail abnormalities is vital for early detection of systemic diseases. Moreover, this research enhances patient education regarding nail health, empowering individuals to recognize signs of abnormalities and seek timely medical assistance.

Due to the nature of machine learning algorithms, external data, skin tone, or other dermatological factors unrelated to human nails may or may not be relevant to the use cases. Given the financial limitations associated with the project, the Raspberry Pi 4 Model B was selected as the preferred hardware for the prototype also considering its processing power constraints [18]. As a cost-effective option, it provides a reasonable computing capability for running object detection algorithms. Considering that the hardware was the main bottleneck, Yolov8n was then chosen.

2 METHODOLOGY

Figure 1 depicts the conceptual framework. The process involved acquiring a Nail Abnormality Dataset, which was then annotated using instance segmentation through Roboflow. To enhance the dataset's diversity and improve the model's generalization, various data augmentation techniques for three version of dataset were applied using Roboflow. The custom YOLOv8n model was then trained using the pre-processed and augmented dataset. Subsequently, the model's performance was evaluated using several metrics. The mean Average Precision (mAP) was calculated to compare the model's performance with different augmentation techniques. The confusion matrix combined with Precision-Recall curve provided insights into the model's precision and recall for each nail abnormality class. Lastly, the F1-Confidence evaluation

ICBET 2024, June 14–17, 2024, Seoul, Republic of Korea

ACM ISBN 979-8-4007-1762-8/24/06
https://doi.org/10.1145/3678935.3678956

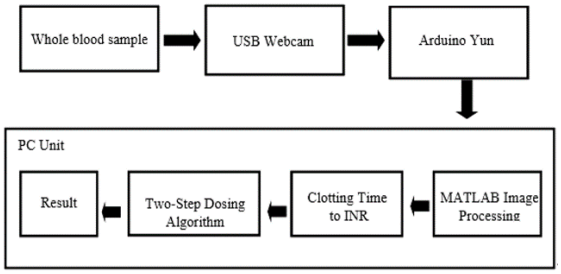

Figure 1: Conceptual Framework

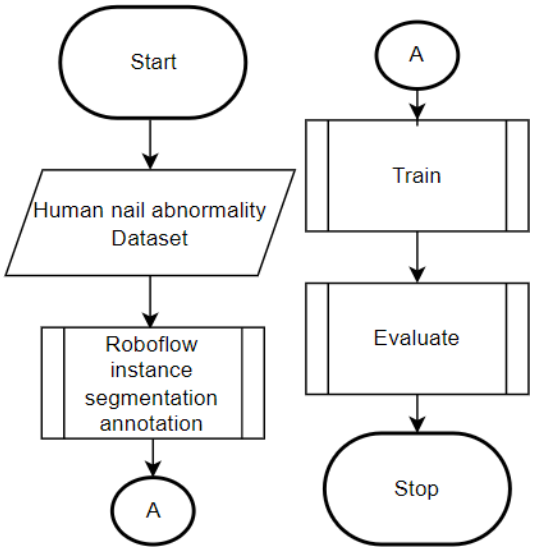

Figure 2: Modelling Procedure

Figure 3: The Three Nail Abnormalities

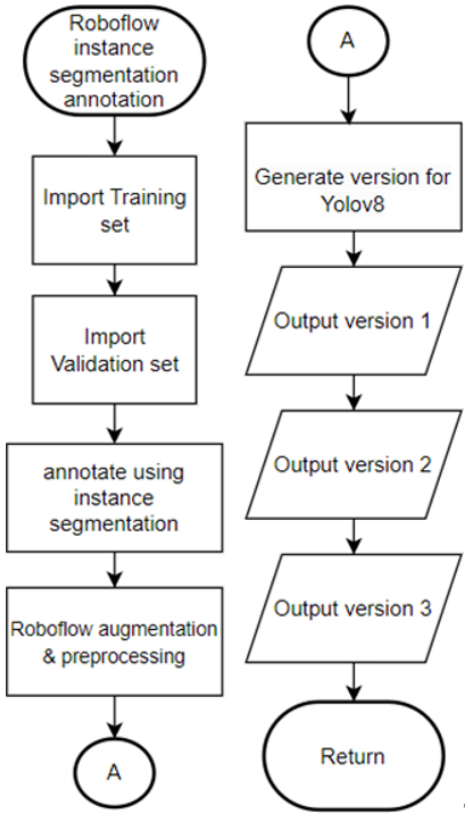

Figure 4: Annotation Procedure

measured the model's overall performance across different confidence levels and choose the best-balanced confidence threshold. The final output of this research was a custom nail abnormality instance segmentation model for Spoon nail, Splinter Haemorrhage and Terry's nail.

2.1 2.1 Modelling Procedure

Figure 2 depicts modelling procedure of the proposed system. Initially, the modelling process involves gathering images of human-nail abnormalities, specifically Spoon nail, Splinter Haemorrhages, and Terry's nail. The data processing phase includes tasks like image augmentation and labelling. Finally, the model undergoes training and evaluation.

2.2 Data Gathering

The characteristics of the Spoon nail is the spoon-shaped nail. In extreme cases, the tip of the nail is almost facing upwards [19]. The characteristics of Splinter Haemorrhages is a wood splinter-like longitudinal streaks that are sometimes dark to red-brown [20].Lastly, the feature of Terry's nails is that almost all the nail is washed out in white to frosty glass-like feature and doesn't have the moon shape near the cuticle [19].

To compile the dataset, validation and testing images were gathered from kaggle and Dermnetnz.org a reliable source for dermatological images [21], [22].

2.3 Data Processing

The images were then imported and annotated using Roboflow annotation editor. Additionally, Roboflow was used to augment the dataset because it provides diverse and consistent augmentation techniques, automates the process and it integrates well with Yolov8. Furthermore, Yolov8 *ultralytics=8.0.142* does not support inference augmentation and test-time augmentation for segmentation models yet [23], [24].

Figure 5: Roboflow annotation

Using Roboflow's annotation tools, we meticulously drew polygons around the regions of interest in our images. This enabled us to define the exact contours and intricate details of the nails. In addition, we carefully selected the validation set images and imported them separately to override Roboflow's automatic training/validation split feature to ensure good representation of each class.

Table 1 shows three versions of the dataset were generated to explore and identify the most effective combination of augmentation parameters. The augmentations in Version 1 include image level augmentations only (Flip: Horizontal, Vertical 90°, Rotate: Clockwise, Counter-Clockwise, Upside-Down Rotation: Between -45° and +45°, and Shear: ±20° Horizontal, ±20° Vertical). Version 2 also has similar image level augmentation with Version 1 but with additional Bounding box level augmentation (Bounding Box Rotation: Between -45° and +45°, and Bounding Box Shear: ±20° Horizontal, ±20° Vertical). Lastly Version 3 is similar to Version 2 but with added color level augmentation (Grayscale, Hue, Saturation, Brightness, and Exposure were between -25% to 25% while Blur: Up to 2.5px, and Noise: Up to 5% of pixels).

The images were also resized to 640x640px which is the default input size for Yolov8. By creating multiple augmented datasets, we aimed to systematically assess various augmentation techniques and settings to determine the optimal configuration that yields the best base model. Image level augmentation [25-27] and color augmentation [28] has been proven successful. Meanwhile bounding box augmentation has already been proven in other field [29] it has yet to be used in nail abnormality datasets specially using instance segmentation.

Figure 3 showcases a sample output generated using *Roboflow* mentioned earlier. After each version of the dataset has been generated a quick visual inspection was done to ensure that the augmentation has been applied correctly and the annotations are correct. Furthermore, *Roboflow* offers a class balance feature that calculates the number of instances per class in the training, validation, and testing split, ensuring a balanced representation of classes. *Roboflow* also provides dimension insights, that helps identify image size irregularities that might affect model training. And annotation heatmap ensures good placement of the augmented nail within the image.

Table 2 represents the number of images per class for each version of the dataset. Even though each dataset has the same number of images, the variability in the configuration of augmentation can introduce subtle differences between them. These variations arise due to differences in the types of augmentation techniques used, the intensity or magnitude of augmentation, the order in which augmentations are applied, and the randomness involved in the augmentation parameters.

2.4 Training and Evaluation

The study employed the Yolov8n-segmentation model, acquired from the official website. The training was conducted using *Ultralytics* (version 8.0.142), *PyTorch* Build Stable (version 2.0.1), *CUDA* (version 12.1) with driver (version 531.79) on *Ubuntu* (20.04.6 WSL2). The experiment utilized an *NVIDIA GTX 1070* GPU and a Ryzen 5 5600x CPU for training the model. To simplify the importing of the dataset, we integrated *Roboflow* (version 1.1.2) into our *Conda* (version 23.3.1) with *Python* (version 3.10.12) environment. For the hyper-parameter configuration, *imgsz=640*, *conf=0.5*, *epochs=250*, *patience=50*, *cos_lr=True*, while other values were set to default.

The study employed the Yolov8n-segmentation model, acquired from the official website. The training was conducted using *Ultralytics* (version 8.0.142), *PyTorch* Build Stable (version 2.0.1), *CUDA* (version 12.1) with driver (version 531.79) on *Ubuntu* (20.04.6 WSL2). The experiment utilized an *NVIDIA GTX 1070* GPU and a Ryzen 5 5600x CPU for training the model. To simplify the importing of the dataset, we integrated *Roboflow* (version 1.1.2) into our *Conda* (version 23.3.1) with *Python* (version 3.10.12) environment. For the hyper-parameter configuration, *imgsz=640*, *conf=0.5*, *epochs=250*, *patience=50*, *cos_lr=True*, while other values were set to default.

Table 1: Augmentation Information

	Image level	Bounding Box Level	Color Level
Version 1	**Flip Rotate Shear**	NA	NA
Version 2	**Flip Rotate Shear**	**Bounding Box Rotation Bounding Box Shear**	NA
Version 3	**Flip Rotate Shear**	**Bounding Box Rotation Bounding Box Shear**	**Grayscale Hue Saturation Brightness Exposure Blur Noise**

Figure 6: Sample Augmented Images

Table 2: Dataset Information

Dataset Information			
Nail Abnormality	AugmentedTraining images	UnaugmentedValidation images	Unaugmented Test images
Splinter Haemorrhage	1200	65	10
Terry's Nail	1200	65	10
Spoon Nail	1200	65	10
Healthy Nail	1200	65	10

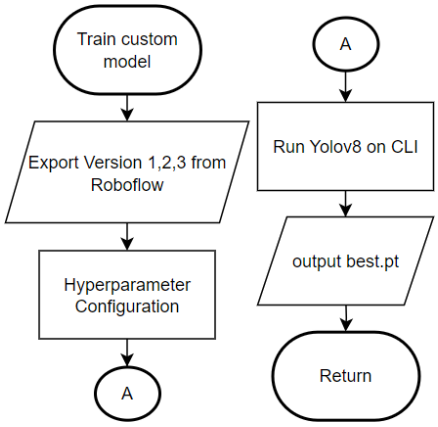

Figure 7: Training Flowchart

3 Results and Discussion

For validation, the confidence and Intersection over Union (IoU) values for the normalized bounding box confusion matrix are currently fixed at 0.25 and 0.45 respectively. he Precision and Recall curve (PRC) and the mean Average Precision (mAP) on the other hand were configured at confidence threshold of .50 and Intersection Over Union (Iou) of 0.50 as shown in Figure 8.

After the training process, the three models were compared using the formula (1) of Mean Average Precision (mAP) for each class to determine the best base model as shown in Figure 9. Subsequently the confusion matrix and the precision-recall curve were used to further evaluate the chosen model. These evaluation techniques provided valuable insights into the models' performances, enabling researchers to identify the most effective model for the specified nail abnormality detection task. Additionally, F1- confidence curve will be used to balance both precision and recall, which hold critical significance in medical diagnosis. Furthermore, we deployed the trained model on a Raspberry Pi 4 Model B for implementation.

$$mAP = \sum_{n}^{k=1} (AP_k) \tag{1}$$

The data table compares the Mean Average Precision (*mAP*) scores of three different versions (Version 1, Version 2, and Version 3. The data suggest that Healthy and Splinter haemorrhage class were impacted negatively using Image level and Bounding box level augmentation (version 2). But has dramatic increase over version 3 compared to version 2. The Spoon nail class also had similar effects but very minimal with only 0.001 increments and decrements. Based on the provided *mAP*@50 scores, it appears that colour level augmentation might not have been as beneficial for Terry's Nail class as other classes in the dataset.

Overall, Version 3 had the best *mAP* among the three versions of the nail abnormality detection model. It achieved an overall *mAP*@50 of 0.896, which is the highest compared to Version 1 and Version 2.

In the normalized confusion matrix of *YOLOv8*, the background class is included by default as it plays a crucial role in the YOLO algorithm. *YOLOv8* considers any region in an image where there is no object as the 'background.' This means that when the model makes predictions, it not only detects and classifies objects of interest but also identifies areas with no objects, labelling them as background regions.

The Version 3 model displayed strong performance in correctly identifying "Healthy Nail" instances with a 95% true positive rate (TPR). However, it struggled with false positive rates (FPR), misclassifying 3% as "Spoon Nail," 18% as "Terry's Nail," and 2% as "Spoon Nail," highlighting an imbalance in precision and recall. For "Splinter Hemorrhage," the model achieved a 94% TPR but exhibited

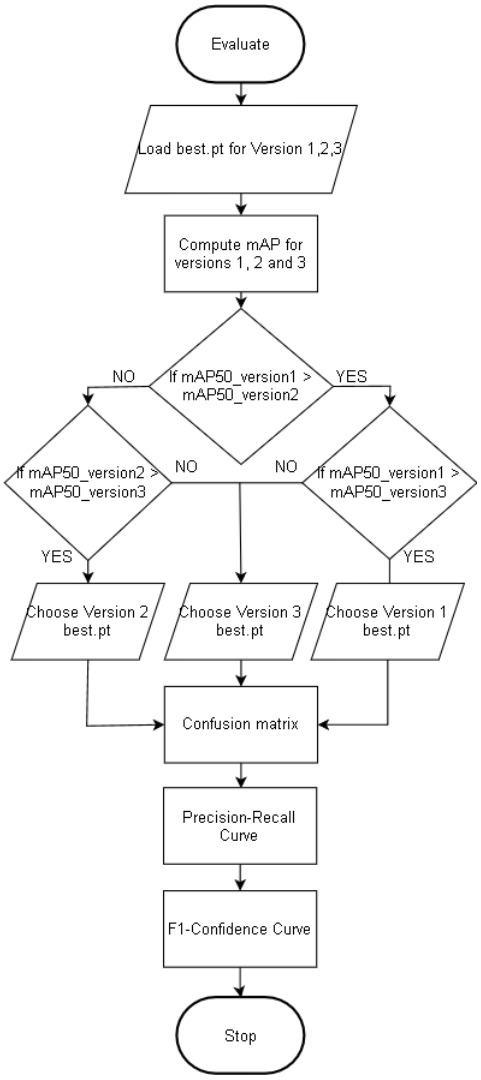

Figure 8: Evaluate Flowchart

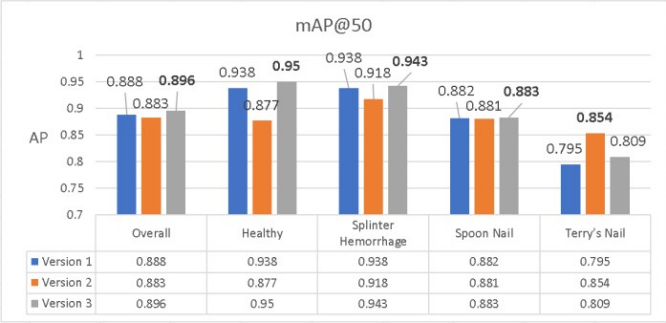

Figure 9: Mean Average Precision (MAP) Comparison

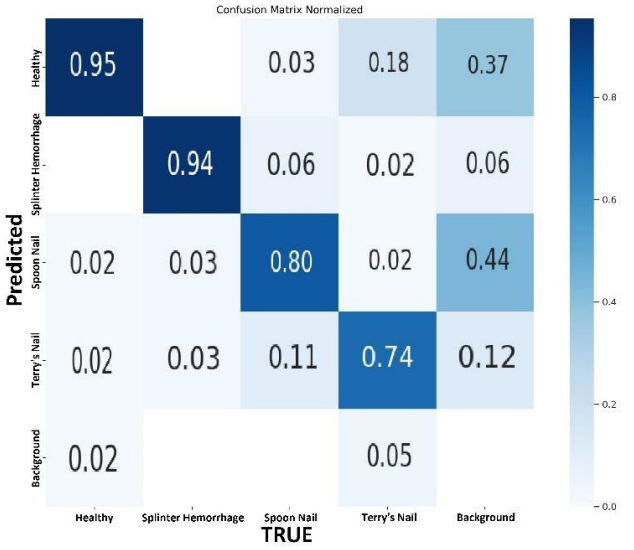

Figure 10: Version 3 Normalized Confusion Matrix

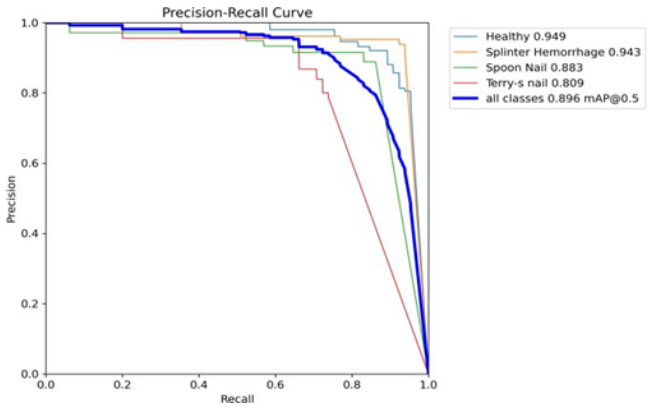

Figure 11: Version 3 Mask Precision-Recall Curve mAP50

confusion by producing false positive detections for "Terry's Nail" and "Spoon Nail." In the case of "Spoon Nail," it performed well with an 80% TPR but had FPRs for "Terry's Nail," "Splinter Hemorrhage," and "Healthy Nail." Similarly, for "Terry's Nail," the model achieved a 74% TPR but showed FPRs for "Background," "Spoon Nail," "Splinter Hemorrhage," and "Healthy Nail," indicating challenges in distinguishing it from other classes as shown in Figure 10.

Using precision-recall curve visualization at mAP50, we further assessed the performance of the nail abnormality detection model for different classes. Based on the data, the *Terry's Nail* class has very low recall compared to the other class. While the precision is acceptable, indicating that when the model predicts an instance as "*Terry's Nail*," it is correct 80% of the time, the recall score suggests that the model might not be capturing all instances of "Terry's Nail" present in the dataset.

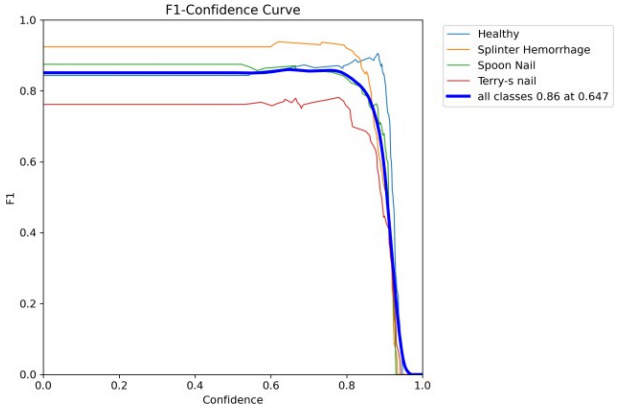

Figure 12: Version 3 Mask F1-Confidence Curve

	Class	n(truth)	Classified	Accuracy	Precision	Recall
Version 3	Healthy	65	82	92.51%	0.76	0.95
	Splinter Hemorrhage	65	67	96.31%	0.91	0.94
	Spoon Nail	65	58	92.99%	0.90	0.80
	Terry's nail	65	60	89.33%	0.80	0.74
Version 3 balanced	Healthy	65	78	92.91%	**0.79**	0.95
	Splinter Hemorrhage	65	64	**96.64%**	**0.94**	0.92
	Spoon Nail	65	59	91.04%	0.85	0.77
	Terry's nail	65	55	**89.55%**	**0.84**	0.71

Figure 13: Version 3 Balanced Values

Using the F1-score a confidence threshold of 0.647 provided the most balanced performance in terms of precision and recall for the nail abnormality segmentation task as shown in Figure 12.

Using a confidence threshold of 0.647 from the F1- confidence sweep we balanced the Precision and Recall of Version 3. With the balanced Version 3 we get a slight increase of 0.03 for the Healthy and Splinter Haemorrhage, 0.04 for the Terry's nail. However, Spoon nail decreased by 0.05.

Class-specific precision was calculated using formula (2). Calculating precision per-class is essential in this application as it allows us to evaluate the model's accuracy for individual classes, pinpoint strengths, and weaknesses, and assess the impact of misclassifications on specific categories.

$$\text{Precision} = \frac{True\ Positive}{True\ Positive + False\ Positive} \tag{2}$$

For the class-specific recall values formula (3) was used to ensure that the model is not biased towards the majority class and provides insights into areas where improvements may be needed, contributing to a more comprehensive understanding of the model's effectiveness across all categories

$$\text{Recall} = \frac{True\ Positive}{True\ Positive + False\ Negative} \tag{3}$$

4 Conclusions and Recommendation

In conclusion, we evaluated three versions of a custom YOLOv8n model for detecting nail abnormalities using different augmentation techniques. We observed that each class exhibited distinct responses to various augmentation techniques. This indicates that the impact of augmentation on model performance varies depending on the specific characteristics of each nail abnormality class.

References

[1] V. Saranya and A. Ranichitra, "Image Segmentation Techniques To Detect Nail Abnormalities," *Int. J. Comput. Technol. Appl.*, vol. 8, no. 4, pp. 522–527, 2017.

[2] C. B. Yelverton and J. L. Jorizzo, "Nail Signs of Systemic Disease," in *Dermatological Signs of Internal Disease*, Fourth., Elsevier, 2009, pp. 365–373.

[3] R. Rajan, "CENTRAL ASIAN JOURNAL OF MEDICAL AND NATURAL SCIENCES 2022 : Special Issue " Medical Ethics and Nail Disease Detection and Classification Using Deep Learning," no. May, 2022.

[4] R. Bawankule, V. Gaikwad, I. Kulkarni, S. Kulkarni, A. Jadhav, and N. Ranjan, "Visual Detection of Waste using YOLOv8," *Int. Conf. Sustain. Comput. Smart Syst. ICSCSS 2023 - Proc.*, no. Icscss, pp. 869–873, 2023, doi: 10.1109/ICSCSS57650.2023.10169688.

[5] P. Li, "Research on RGB-D SLAM Dynamic Environment Algorithm Based on YOLOv8," *Proc. 2023 IEEE 3rd Int. Conf. Inf. Technol. Big Data Artif. Intell. ICIBA 2023*, vol. 3, no. Iciba, pp. 1038–1044, 2023, doi: 10.1109/ICIBA56860.2023.10164898.

[6] R. Nijhawan, R. Verma, Ayushi, S. Bhushan, R. Dua, and A. Mittal, "An integrated deep learning framework approach for nail disease identification," *Proc. - 13th Int. Conf. Signal-Image Technol. Internet-Based Syst. SITIS 2017*, vol. 2018-Janua, pp. 197–202, 2018, doi: 10.1109/SITIS.2017.42.

[7] H. F. Hasya, H. H. Nuha, and M. Abdurohman, "Real Time-based Skin Cancer Detection System using Convolutional Neural Network and YOLO," *Proc. - 2021 4th Int. Conf. Comput. Informatics Eng. IT-Based Digit. Ind. Innov. Welf. Soc. IC2IE 2021*, pp. 152–157, 2021, doi: 10.1109/IC2IE53219.2021.9649224.

[8] S. I. I. C. Imperial, A. L. L. Lucas, and M. V. Caya, "Vehicle Type Classification and Counting Using YOLOv4 Algorithm," *4th IEEE Int. Conf. Artif. Intell. Eng. Technol. IICAIET 2022*, pp. 1–6, 2022, doi: 10.1109/IICAIET55139.2022.9936874.

[9] R. V. Pellegrino, J. H. T. Lacuesta, and C. F. L. Dela Cuesta, "The R. V. Pellegrino, J. H. T. Lacuesta, and C. F. L. Dela Cuesta, "The Effect of Using Augmented Image in the Identification of Human Nail Abnormality using Yolo3," *2023 15th Int. Conf. Comput. Autom. Eng. ICCAE 2023*, pp. 187–192, 2023, doi 10.1109/ICCAE56788.2023.10111315.

[10] C. J. L. Chan, E. J. A. Reyes, N. B. Linsangan, and R. A. Juanatas, "Real-time Detection of Aquarium Fish Species Using YOLOv4-tiny on Raspberry Pi 4," *4th IEEE Int. Conf. Artif. Intell. Eng. Technol. IICAIET 2022*, no. 1, pp. 1–6, 2022, doi:

[11] N. B. Linsangan, J. V. G. Calites, J. T. L. Reyes, G. C. D. Sioson, R. V. Pellegrino, and I. C. Juanatas, "Filipino Sign Language to Text Converter using K-Nearest Neighbor Algorithm," *2022 IEEE 14th Int. Conf. Humanoid, Nanotechnology, Inf. Technol. Commun. Control. Environ. Manag. HNICEM 2022*, no. c, pp. 1–6, 2022, doi: 10.1109/HNICEM57413.2022.10109512.

[12] R. V. Pellegrino, A. C. Tarrobago, and D. L. B. Zulueta, Development of Anemia Cells Recognition System Using Raspberry Pi," *2023 15th Int. Conf. Comput. Autom. Eng. ICCAE 2023*, pp. 198–203, 2023, doi: 10.1109/ICCAE56788.2023.10111486.

[13] R. B. Sanchez, J. Angelo C. Esteves, and N. B. Linsangan, "Determination of Sugar Apple Ripeness via Image Processing Using Convolutional Neural Network," *2023 15th Int. Conf. Comput. Autom. Eng. ICCAE 2023*, pp. 333–337, 2023, doi:10.1109/ICCAE56788.2023.10111204.

[14] J. G. Sinco, N. B. Linsangan, and R. V Pellegrino, "DentIS : Dental Bracing Procedure Information System Using Cosine Metric Algorithm for Image Processing," pp. 2–6, 2019.

[15] A. S. Muhali and N. B. Linsangan, "Classification of Lanzones Tree Leaf Diseases Using Image Processing Technology and a Convolutional Neural Network (CNN)," *4th IEEE Int. Conf. Artif. Intell. Eng. Technol. IICAIET 2022*, pp. 1–6, 2022, doi: 10.1109/IICAIET55139.2022.9936833.

[16] R. S. S. Suliva, C. A. A. Valencia, and J. F. Villaverde, "Classification and Counting of Ships Using YOLOv5 Algorithm," *2022 6th Int. Conf. Commun. Inf. Syst. ICCIS 2022*, pp. 153–158, 2022, doi: 10.1109/ICCIS56375.2022.9998129.

[17] A. N. Yumang, J. F. Villaverde, M. H. C. Tan, and J. K. D. Tulfo, "Bacterial Leaf Blight Identification of Rice Fields Using Tiny YOLOv3," *4th IEEE Int. Conf. Artif. Intell. Eng. Technol. IICAIET 2022*, pp. 1–5, 2022, doi: 10.1109/IICAIET55139.2022.9936825.

[18] P. Sismananda, M. Abdurohman, and A. G. Putrada, "Performance Comparison of Yolo-Lite and YoloV3 Using Raspberry Pi and MotionEyeOS," *2020 8th Int. Conf. Inf. Commun. Technol. ICoICT 2020*, 2020, doi: 10.1109/ICoICT49345.2020.9166199.

[19] A. Oakley and I. Coulson, "Nail terminology," *dermnetnz.org*. https://dermnetnz.org/topics/nail-terminology (accessed Jul. 14, 2021).

[20] A. Manley and A. Oakley, "Splinter haemorrhage," *dermnetnz.org*. https://dermnetnz.org/topics/splinter-haemorrhage (accessed Jun. 10, 2021).
[21] DermNet, "Nail disorders," *dermnetnz.org*. https://dermnetnz.org/topics/nail-disorders (accessed Jun. 02, 2021).
[22] Nail Disease Datasets, Kaggle.com, May 2021. [Online]. Available: https://www.kaggle.com/datasets?search$=$nail+disease.
[23] Ultralytics, "How to use augments in the inference stage of yolov8 segmentation? · issue #3366 · Ultralytics/ultralytics," *GitHub*. https://github.com/ultralytics/ultralytics/issues/3366 (accessed Aug. 24, 2023).
[24] Ultralytics, "Segmentation model do not support augment inference · issue #2419 · Ultralytics/ultralytics," *GitHub*. https://github.com/ultralytics/ultralytics/issues/2419%0A (accessed Aug. 20, 2023).
[25] D. Thapar, G. Jaswal, and A. Nigam, "FKIMNet: A Finger Dorsal Image Matching Network Comparing Component (Major, Minor and Nail) Matching with Holistic (Finger Dorsal) Matching," *Proc. Int. Jt. Conf. Neural Networks*, vol. 2019-July, no. July, pp. 1–8, 2019, doi: 10.1109/IJCNN.2019.8852390.
[26] Y.-C. Liu, Y.-L. Lin, C.-Y. Chou, and C.-S. Fuh, "Identification of Nail Lesions Based on Mask R-CNN Deep Learning Model."
[27] L. Folle *et al.*, "DeepNAPSI multi-reader nail psoriasis prediction using deep learning," *Sci. Rep.*, vol. 13, no. 1, pp. 1–8, 2023, doi: 10.1038/s41598-023-32440-8.
[28] H. Muneera Begum, A. Dhivya, A. J. Krishnan, and S. D. Keerthana, "Automated Detection of skin and nail disorders using Convolutional Neural Networks," *Proc. 5th Int. Conf. Trends Electron. Informatics, ICOEI 2021*, pp. 1309–1316, 2021, doi: 10.1109/ICOEI51242.2021.9452959.
[29] K. Lee, S. Lee, and H. Y. Kim, "Bounding-box object augmentation with random transformations for automated defect detection in residential building façades," *Autom. Constr.*, vol. 135, no. July 2021, p. 104138, 2022, doi: 10.1016/j.autcon.2022.104138.